Excitation Energy Migration of Acridine Orange Intercalated into Deoxyribonucleic Acid Thin Films

Fuyuki Ito,* Toshifumi Kakiuchi, and Toshihiko Nagamura*

Department of Applied Chemistry, Faculty of Engineering, Kyushu University, 744 Motooka, Nishi-ku, Fukuoka 819-0395, Japan

Received: December 19, 2006; In Final Form: March 7, 2007

The excitation energy migration of acridine orange (AO) immobilized in deoxyribonucleic acid (DNA) thin film was investigated by time-resolved fluorescence and fluorescence anisotropy decay measurements. Polyvinylalcohol (PVA) was used as a reference matrix. The absorption and fluorescence spectra indicated that the molecular aggregation was depressed in DNA thin films rather than in PVA thin films. Time-resolved fluorescence spectra of AO in DNA films suggested effcient energy transfer from monomer to trap sites, dimers, or aggregates. Fluorescence lifetime of AO in DNA films was decreased with increasing fractions of AO, which suggested efficient energy migration between intercalated AOs. The fluorescence anisotropy measurements directly supported the efficient energy migration between intercalated AOs. These findings indicate that the double-helix DNA contributes to the efficient energy migration between intercalated dyes.

Introduction

The interactions between the cationic organic dyes and deoxyribonucleic acid (DNA) have been widely studied in terms of the biological and physical chemistry to detect DNA using their fluorescence.[1] The cationic dyes such as ethidium bromide (EB), profravin (PF), and acridine orange (AO) can be easily intercalated into the base pairs of DNA, which enhanced the fluorescence intensity of the dyes.[2−8] The enhancement mechanism of the fluorescence intensity has been reported in aqueous solution by the fluorescence lifetime measurements.[9] This is attributed to reduction in the rate of the nonradiative path from the excited state, suggesting restricted mobility of the intercalated dyes.[6] The fluorescence spectra and fluorescence lifetime of the dyes are very sensitive to the environments of the dyes; thus it can be used as a probe to investigate the intermolecular interaction between the dyes and DNA.

DNA can organize various organic molecules because it has a characteristic structure, such as the double strand with hydrogen bondings, and molecules can intercalate into the stacking base pairs. To use this characteristic behavior, the DNA can be used as a block for construction of one-dimensional assemblies. There are several reports about the photoinduced electron transfer or energy transfer between intercalated molecules.[10−14] In particular, the efficient excitation energy transfer occurs between the intercalated dyes along the chain.[15,16] Kubota et al.[15] reported that the fluorescence polarization of AO in DNA aqueous solution at steady state measurements was decreased with increasing the fraction of AO in DNA, which resulted in the excitation energy transfer between the intercalated AO molecules. They also analyzed the fluorescence decay curves of AO in DNA aqueous solution based on the Förster type energy transfer. The average distance between two nearest intercalated molecules is about 25−35 Å. Femtosecond laser spectroscopy, such as pump−probe and fluorescence up-conversion measurements, is adapted to reveal the much faster phenomena in dyes−DNA system.[17,18] The pump−probe experiment for the AO−DNA system pointed out a delocalization of the electronic excitation over neighboring dyes separated by two base pairs (ca. 10 Å) in the DNA stack.[17] These findings suggested that the excited state dynamics is different of the observed time domain. These reports are only for the fluorescence properties of the dyes intercalated into DNA in the aqueous solution system. There is no report for the excited-state dynamics of the dyes in DNA thin films. It is important to understand detailed mechanism in the excited molecules in solid films to take into account of the application for the devices based on the DNA matrix.

We have reported the application of highly sensitive fluorescence measurements of dyes in DNA films deposited on a metal film to high-performance gas sensing.[19] Thin DNA films attached in the gas cell were excited under surface plasmon resonance (SPR) condition in a Kretschmann configuration. By using the SPR, the fluorescence intensity is enhanced by the electric field of evanescent light. The fluorescence intensity decreased in the presence of ppb ∼ ppm order nitrogen oxide (NO_x) by the photoinduced electron transfer reaction (redox reaction). The response time and sensitivity for the changes of the fluorescence intensity in DNA film was superior to that in a polyvinyl alcohol (PVA) film. It is explained by the difference of the molecular dispersibility in DNA and PVA. DNA can homogeneously disperse the cationic dyes by the intercalation. The detailed mechanism of high performance in the DNA thin films is not fully clarified yet.

In this paper, to elucidate the excited state dynamics of AO intercalated into DNA thin films, we measured the absorption and fluorescence spectra, time-resolved fluorescence spectra, and fluorescence lifetime. In particular, the energy transfer or energy migration between AO molecules was evaluated by the fluorescence anisotropy decay measurement which is a powerful technique to clarify the transient behavior within the same molecules in the molecular assemblies[20] and solid or film[21] systems. We use PVA as a reference matrix to clarify the effect of molecular dispersion on the fluorescence properties of AO.

* Address correspondence to either author. For F.I.: phone, +81-92-802-2880; fax, +81-92-802-2880; e-mail, f-ito@cstf.kyushu-u.ac.jp. For T.N.: phone, +81-92-802-2878; fax, +81-92-802-2880; e-mail, nagamura@cstf.kyushu-u.ac.jp.

10.1021/jp0687495 CCC: $37.00
Published on Web 04/18/2007

SCHEME 1: Molecular Structure of AO

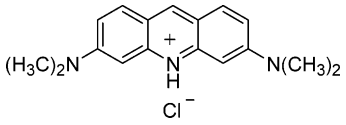

Experimental Procedures

Sample Preparation. AO (Aldrich) (Scheme 1) was used as received without further purification. DNA sodium salt from salmon spermary (Wako Pure Chemicals) was used. Poly(vinyl alcohol) (PVA) purchased from Tokyo Chemical Industry was used without further purification. The DNA concentration in ion-exchanged and distilled water was fixed to 1×10^{-2} mol dm^{-3} (0.66 wt %). To change the AO molecular fraction in the films, concentrations of AO in DNA aqueous solutions were changed from 1×10^{-5} to 1×10^{-3} mol dm^{-3}. The ratios of AO to DNA were 1/50, 1/100, 1/200, 1/300, 1/500, 1/1000, and 1/2000 per base pair, which correspond to the weight fraction of 0.0111, 0.0056, 0.0028, 0.0019, 0.0011, 0.00056, and 0.00028, respectively. Thin films were prepared by spin coating onto a quartz plates. The coated films were dried under vacuum condition at 40 °C for 24 h. Thickness of the film was 50 nm determined by AFM measurements. To clarify effect of intercalation into DNA, we measured the absorption and fluorescence spectra of AO in PVA matrix as a reference. The PVA films doped with AO as a reference sample were prepared by a procedure similar to that for DNA films under the same weight fraction. In this paper, to simplify comparison of concentration between in DNA and PVA film, we describe the ratio AO/PVA corresponding to AO/DNA at the same weight fraction.

Measurements. UV−Vis absorption spectra were measured by Hitachi U-4100 spectrometer. Fluorescence spectra were recorded by Hitachi F-4500 fluorescence spectrophotometer. Fluorescence lifetimes were measured by a single-photon counting method using a streakscope (Hamamatsu Photonics, C4334-01). The sample solutions were excited with SHG (λ = 400 nm) of a mode-locked Ti:sapphire laser (Spectra-Physics, Tsunami, fwhm: 1.5 ps) equipped with a pulse selector and a harmonic generator. The laser beam incidents from the substrate side of the sample under the attenuated total reflection condition via a prism. The fluorescence decays were measured with magic-angle emission polarization to avoid an effect on it in the decay profiles. Time-resolved fluorescence anisotropy was obtained by changing the detection polarization on the fluorescence path parallel or perpendicular to the polarization of the excitation light. The anisotropy decays then were calculated as follows:

$$r(t) = \frac{I_{VV}(t) - GI_{VH}(t)}{I_{VV}(t) + 2GI_{VH}(t)} \quad (1)$$

where $I_{VV}(t)$ (or $I_{VH}(t)$) is the fluorescence decay when the excitation light is vertically polarized and only the vertically (or horizontally) polarized portion of fluorescence is detected, denoting that the first and second subscripts represent excitation and detection polarization, respectively. The factor G is defined by $I_{VV}(t)/I_{VH}(t)$, which is equal to the ratio of the sensitivities of the detection system for vertically and horizontally polarized light. The G factor of our detection system was 0.9. The polarized angle of excitation light was adjusted by using the Berek compensator (Newfocus Model 5540). All experiments were carried out at room temperature.

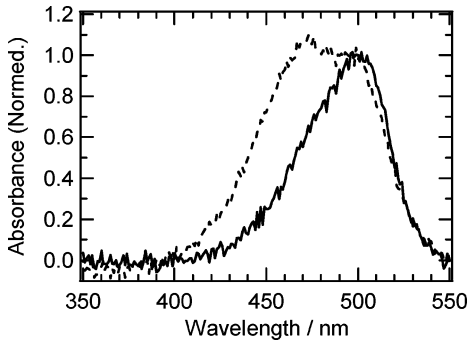

Figure 1. Absorption spectra of AO in DNA (full line) and in PVA (broken line) thin films. The ratio of AO matrix is 1/100 in both cases.

Results and Discussion

Steady State Absorption and Fluorescence Propeties. Figure 1 shows steady state absorption spectra of AO in DNA and PVA thin films. The molar fraction of AO in each films was 1/100, which is converted to 1×10^{-5} mol dm^{-3} in the solution. In the DNA film, the absorption band shows a peak around 492 nm with a small shoulder at 470 nm. The spectral feature agrees with the absorption spectrum of AO in dilute aqueous solution;[5,22,23] therefore the AO is concluded to be solubilized (intercalated) as monomer species in the DNA film. It is indicated that the DNA matrix homogeneously disperse AO molecules by the intercalation between the base pairs. The absorption spectrum of AO in PVA film, on the other hand, showed the absorption peak shift to around 470 nm as shown by the dotted line in Figure 1. No change of the absorption spectrum was observed with decreasing the fraction of AO in PVA. AO molecules can easily aggregate with increasing concentrations in aqueous solutions larger than 1×10^{-4} mol dm^{-3}.[22,23] The absorption peak shifted to the blue with increasing solution concentrations, which was ascribed to the H-dimer.[24] Stomphorst et al. reported that Erythrosin B can be aggregated by increased local concentrations due to evaporation during the spin-coating process even less than 5×10^{-5} mol g^{-1} in solution.[25] Therefore AO molecules are dispersed as aggregated forms in the PVA film even in spin-coated films from a low concentration solution. The absorption properties of AO are clearly different in DNA and PVA matrixes even at the same molecular fraction.

Figure 2a shows the fluorescence spectra of AO with various ratios in DNA films excited at λ = 490 nm. The fluorescence peak was observed around 526 nm which is identical to the literature value.[13,15,26,27] Increasing the fraction of AO in DNA, the fluorescence peaks shifted to longer wavelength by 4 nm, which is most probably caused by the reabsorption by AO. The drastic change of the fluorescence band was not observed in the case of the DNA films. Inset of Figure 2a shows the relation between the fluorescence intensity and weight fraction. The linearity of the fluorescence intensity against the weight fraction indicates that AO molecules were dispersed with very weak interaction between the base pair. Figure 2b shows the fluorescence spectra of AO in PVA films excited at λ = 490 nm with various weight fractions. In the case of 1/1000 ratio, the fluorescence band shows a peak around 512 nm. Increasing of the AO fraction, the peaks shifted to the red by 8 nm, and the fluorescence band became broader toward a longer wavelength region (>560 nm). Buildup of the new emission band at longer wavelength region can be ascribed to formation of excited dimer or aggregated species with increasing the AO contents.[28−30] The existence of dimer species of AO in the PVA films is clearly shown by absorption spectrum depicted in Figure 1. The fraction

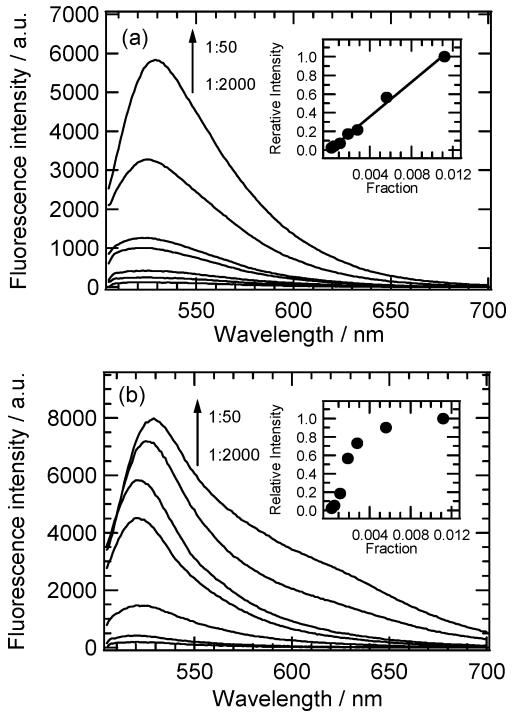

Figure 2. Fluorescence spectra of AO in (a) DNA and (b) PVA thin films excited at 490 nm as a function of ratio. Inset: weight fraction dependence of the peak fluorescence intensity.

dependence of the fluorescence intensity, shown in the inset of Figure 2b, became saturated around the ratio of ca. 1/300. The static quenching occurs in the PVA matrix caused by the aggregated AOs. The steady state absorption and fluorescence spectra thus indicate that the molecular aggregation is markedly depressed in the DNA thin films as compared with that in the PVA thin films.

Time-Resolved Fluorescence Measurements. The excited state dynamics of AO in DNA films were investigated by time-resolved fluorescence and fluorescence lifetime measurements. Time-resolved fluorescence spectra obtained by $\lambda = 440$ nm picosecond laser pulse excitation are shown in Figure 3. The spectra were smoothed in order to blaze the peak position. In the case of AO/DNA = 1/50 (Figure 3a), the fluorescence maximum is located around 530 nm in early time after excitation, which corresponds to the peak obtained by the steady state measurements. This fluorescence spectrum is assigned to the monomer one. At longer time region, the fluorescence spectra were changed with the maximum locating around 550 nm after the 5 ns. The fluorescence spectrum observed at more than 5 ns after the excitation was not clear by the steady state measurements. It can be assigned to the emission from the trace trap sites of AO monomer or dimer fluorescence in the analogy to the time-resolved studies in Langumuir−Blogett (LB) monolayer films reported by Tamai and Yamazaki.[31,32] In the case of AO/DNA = 1/1000, on the other hand, the fluorescence peak is located around 530 nm in early time after excitation. The peak wavelength and the fluorescence band shape did not change even at more than 10 ns after the excitation. It is indicated that only one emissive species exists in the AO/DNA = 1/1000 system. Time-resolved fluorescence spectra support that the intercalation into DNA base pairs is very effective to disperse AO molecules homogeneously even in thin films. It is also suggested that the energy transfer occurs from monomer to the trace trap sites, to dimer, or to aggregates. The time-resolved fluorescence spectra of AO in PVA films show different shapes because AO molecules are easily aggregated in the PVA matrix

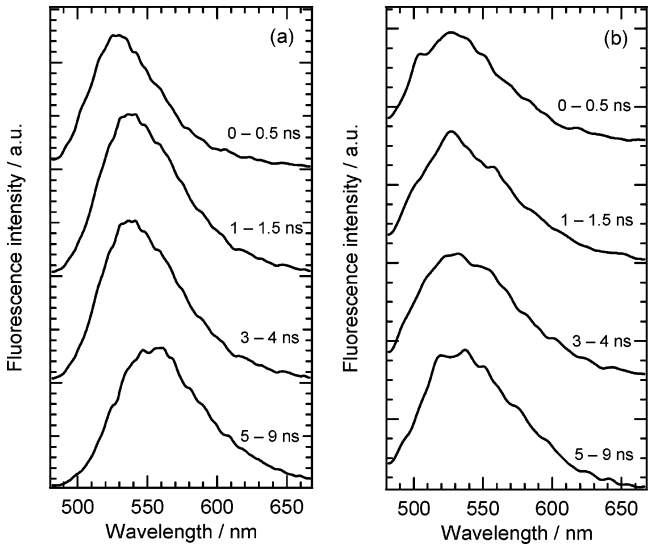

Figure 3. Time-resolved fluorescence spectra of AO in DNA thin film excited at 440 nm by ps laser pulse. The spectra were smoothed in order to blaze the peak position. The time in the figures indicates delay time after the excitation. The ratios of AO to DNA are (a) 1/50 and (b) 1/1000.

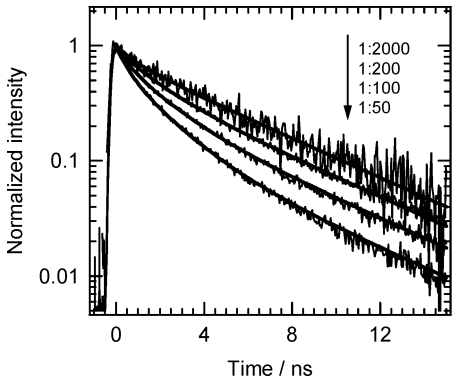

Figure 4. Fluorescence decay curves of AO in DNA thin films excited at 440 nm by picosecond laser pulse. The ratios are indicated in the figure. The solid lines are the fitting results based on the triphasic decay with time constant of 0.45, 1.70, and 5.14 ns.

(see Supporting Information). The fluorescence spectra of AO in PVA film (1/50) showed the long wavelength region at 5 ns after the excitation, which originates from higher aggregates of AO with long lifetime.[30] The fluorescence behavior in PVA matrix is essentially different from that in DNA matrix. However, the spectral shape in the case of AO/PVA with molar ratio of less than 1/500 is identical to the monomer emission. It is indicated that the AO molecules are relatively dispersed in PVA film at low molecular fractions.

Figure 4 shows fluorescence decay curves of AO in DNA thin film excited at $\lambda = 440$ nm and monitored at $\lambda > 500$ nm. The fluorescence decay becomes faster with increasing the AO fraction in DNA matrix, indicating the energy transfer from monomer to trace trap site, to dimer, or to aggregates sites as mentioned above. The fluorescence decay curves were analyzed with three exponential decays. Three components were necessary to get best curve fittings. The fitting results are summarized in Table 1. Time constants of the three components (τ_1, τ_2, and τ_3) were fixed at 0.45, 1.70, and 5.14 ns to compare the relative contribution of the three components, which are well fitted on the fluorescence decay curves of all molecular fractions in the films. The fluorescence lifetime of AO in aqueous solution and in DNA aqueous solution are 1.84 and 5.04 ns, respectively.[15,17]

TABLE 1: Fluorescence Lifetime (τ) and Amplitude (A) Obtained from the Three Exponential Least-Square Fitting of the Decay Curves of AO in DNA Films

ratio	A_1 (τ_1/ns)	A_2 (τ_2/ns)	A_3 (τ_3/ns)
1/2000	0.13 (0.45)	0.19 (1.70)	0.70 (5.14)
1/1000	0.13 (0.45)	0.21 (1.70)	0.68 (5.14)
1/500	0.14 (0.45)	0.28 (1.70)	0.60 (5.14)
1/300	0.14 (0.45)	0.34 (1.70)	0.53 (5.14)
1/200	0.13 (0.45)	0.39 (1.70)	0.49 (5.14)
1/100	0.16 (0.45)	0.48 (1.70)	0.34 (5.14)
1/50	0.28 (0.45)	0.54 (1.70)	0.18 (5.14)

The elongation of the lifetime in the DNA aqueous solution is attributed to depression of the nonradiative decay channel due to the restriction of molecular motion by intercalation. In thin films, when the fraction of AO is increased, the amplitude of the second component with $\tau_2 = 1.75$ ns is increasing and that of the third component with $\tau_3 = 5.14$ ns is decreasing. The amplitude of the component with $\tau_1 = 0.45$ ns which is shorter than the S_1 lifetime of AO is almost constant for the fraction less than 0.005. The τ_3 component can be assigned to the fluorescence lifetime of monomer AO, because the τ_3 is identical to the AO in DNA aqueous solution. The τ_2 component is considered to be the time constant related to the excitation energy transfer between AO monomers, and then the excitation is quenched at the trace trap sites. The variation in amplitude of the τ_1 component can be caused by a possible very effective energy migration between the nearest-neighbor dyes and/or by contribution of the small amount of dimer species as a quenching site in the DNA films. The multiexponential decay leads to various relaxation pathways of the excited AO. The experimental results suggest that the nonradiative relaxation pathways in AO fluorescence are energy migrations to a lower energy site. These phenomena have been reported in the case of LB monolayer films by the time-resolved fluorescence studies about oxacyanine, rhodamine B, fluorine, pyrene, and so on.[32,33] They have found that the LB film is characterized by (1) non-homogeneous distribution of chromophores, (2) formation of dimers and/or aggregates of dyes in molecular cages depressed by the matrix, and (3) the energy migration between dyes located in the same layer. We have observed amplified quenching of carbazolyl derivatives in the LB monolayer films by a trace amount of acceptor (quencher).[34−36] The degree of quenching was increased with increasing the fraction of chromophores in the system. The quenching is followed by the efficient energy migration between the calbazolyl derivatives, which are well-ordered with the assistance of the film structures. The excited state property of the present DNA system is similar to the LB monolayer system. The characteristic structure of DNA can disperse and orient dyes intercalated between the base pairs. The alignment of the dyes results in the amplified quenching followed by the efficient energy migration. We observed first the excitation energy migration process between the intercalated dyes and quenching of the excited states depending on the fraction of the dye in the DNA thin films.

In order to compare the excited state dynamics of AO in DNA thin film, we also measured the fluorescence lifetime in PVA films. The fluorescence decay curves are shown in Figure S2 of Supporting Information. The fluorescence lifetime and amplitude obtained from the least-square fitting assumed by three or two exponential decays are listed in Table 2. In the case of ratio higher than 1/300, the fluorescence decays are well-reproduced by three exponential decays with $\tau = 0.41$, 1.79, and 9.64 ns. The $\tau = 9.64$ ns component probably can be assigned to the higher aggregated species which was reported previously.[30] This component is essentially different from

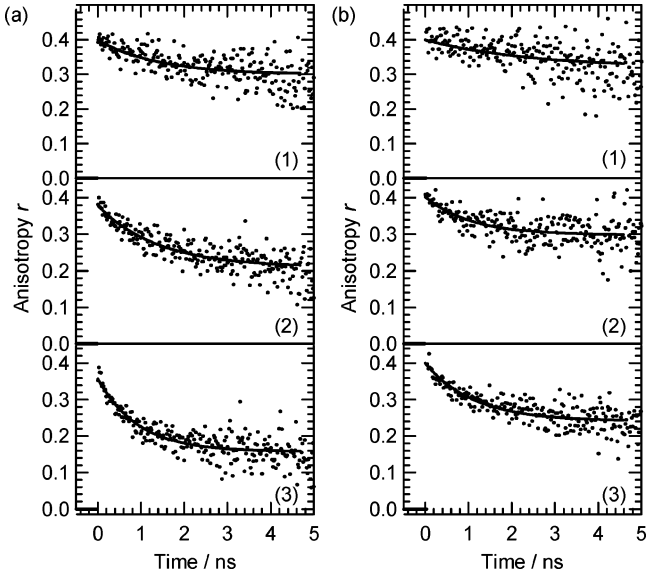

Figure 5. Fluorescence anisotropy decay curves $r(t)$ of AO in (a) DNA and (b) PVA thin films excited at 440 nm by picosecond laser pulse. The ratios are (1) 1/500, (2) 1/100, and (3) 1/50. The solid lines are the fitting results based on the single-exponential decay (see text). The ratios AO/PVA correspond to AO/DNA at the same weight fraction.

TABLE 2: Fluorescence Lifetime (τ) and Amplitude (A) Obtained from the Three Exponential Least-Square Fitting of the Decay Curves of AO in PVA Films

ratio[a]	A_1 (τ_1/ns)	A_2 (τ_2/ns)	A_3 (τ_3/ns)
1/2000	0.40 (1.76)	0.58 (4.60)	–
1/1000	0.40 (1.40)	0.58 (4.40)	–
1/500	0.47 (1.17)	0.51 (4.30)	–
1/300	0.10 (0.41)	0.71 (1.79)	0.15 (9.64)
1/200	0.27 (0.41)	0.59 (1.79)	0.11 (9.64)
1/100	0.45 (0.41)	0.46 (1.79)	0.09 (9.64)
1/50	0.56 (0.41)	0.40 (1.79)	0.08 (9.64)

[a] The ratios AO/PVA correspond to AO/DNA at the same weight fraction.

fluorescence lifetime obtained from the case of AO in the DNA systems. In the case of the ratio lower than 1/500, on the other hand, the fluorescence decay curves are reproduced by the double-exponential function with almost the same lifetime and amplitude. The two components of decays may be originated from heterogeneity of the films. It is clear that the photophysical behavior of AO is different in the DNA and in the PVA matrix.

Fluorescence Anisotropy Decay Process of AO in DNA Thin Film. The fluorescence decay analysis alone is not enough to elucidate the energy migration process in the films. To directly clarify the excitation energy transfer dynamics, fluorescence depolarization method was applied. Energy migration in these arrays leads to a reorientation of the transition dipole moments and thus leads to decrease of the fluorescence polarization anisotropy, r. The anisotropy decay curve gives a direct relationship with the migration process of the excitation energy.[16,21,28,37] Figure 5 shows fluorescence anisotropy decay of AO in DNA and PVA thin films. Since AO molecules in the thin films are hardly allowed to rotate, the anisotropy decay is caused only by the energy migration. The anisotropy decays consist of monoexponential decay (τ_{dep}) and a constant component (r_∞) from initial anisotropy (r_0) in all cases[38] (where r_∞ is the residual anisotropy value and τ_{dep} is the time constant of depolarization). The time constants for the decay of $r(t)$ are listed in Table 3. In each case, the r_∞ value remained considerably high (0.15∼0.32), which indicates that the rotation of the AO molecule is highly restricted in DNA and PVA matrixes. First

TABLE 3: Fitting Result of the Initial Anisotropy (r_0), Residual Anisotropy (r_∞), and Time Constant of Depolarization (τ_{dep}) of AO in DNA and PVA Films

ratio	r_0	r_∞	τ_{dep}/ns
	AO/DNA		
1/500	0.39	0.30	1.6
1/100	0.38	0.21	1.4
1/50	0.36	0.15	0.9
	AO/PVA[a]		
1/500	0.40	0.32	1.7
1/100	0.40	0.30	1.7
1/50	0.40	0.24	1.7

[a] The ratios AO/PVA correspond to AO/DNA at the same weight fraction.

we discuss the anisotropy decay in the DNA system. The anisotropy decay curves in DNA films are shown in Figure 5a. The r_0 and r_∞ values are decreased with increasing the fraction of AO in DNA. The τ_{dep} value is also decreased with increasing the fraction of AO in DNA. The depolarizing process is completed within 5 ns in all systems. The slight decrement of r_0 obviously indicates that the fast depolarization occurs in the higher concentration by the energy migration within less than 300 ps. The anisotropy decay constant τ_{dep} indicates that the migration occurred more efficiently with increasing AO fraction. The r_∞ value is related to the degree of the energy migration efficiency in the rigid system. The experimental results verify that the energy migration takes place in the DNA films. Next, to compare matrix effect on the energy migration process, the fluorescence anisotropy decays were measured in the PVA matrix. The anisotropy decay curves in PVA films are also illustrated in Figure 5b. The depolarization occurred also in the PVA matrix, which is caused by the energy migration between AO molecules. The initial anisotropy $r_0 = 0.4$ in all systems indicates that the fast depolarizing process dose not exist in the PVA matrix. The residual anisotropy r_∞ in the PVA matrix is decreased with increasing the ratio of AO. The values in PVA matrix are higher than those in DNA matrix at the same ratio. It is thus indicated that the energy migration efficiency in the PVA matrix is lower than that in the DNA matrix. However, the depolarizing time constant τ_{dep}, which did not depend on the ratio of AO in the PVA matrix, is larger than that in DNA system. The PVA does not act as matrix for the efficient energy migration process compared to the DNA one. The fluorescence spectra and fluorescence decay behavior of AO with the fraction higher than 0.0033 indicates the aggregated AO in the films. Thus, the depolarization process is most likely a trapping process to the aggregated AO. The DNA double strand acts as an efficient energy transport system by the intercalation of the dyes. The very small depolarization in the case of AO/PVA = 1/500 indicates that the energy migration rarely occurred and hindrance of rotation of AO in the films. These findings suggest that the migration processes of excitation energy in the DNA system have an advantage over that in PVA system.

Excitation Energy Migration of AO Depending on Molar Fraction in DNA Thin Film. In order to discuss the fraction dependence of the energy migration efficiency in DNA matrix, we calculate the critical distance of the energy transfer. In the Förster theory for energy transfer[39] the critical distance, R_0, is the distance between donor and acceptor at which the rate constant for energy transfer is equal to the sum of rate constants for all other deactivation processes of the donor. The critical distance can be calculated from the following equation[39]

$$R_0 = \sqrt[6]{\frac{8.8 \times 10^{-25} \kappa^2 \Phi_D J}{n^4}} \quad (2)$$

where $n = 1.33$ is the solvent refractive index adapted for water[16] and κ^2 is an orientation factor that depends on the relative orientation of the transition dipoles involved in the donor fluorescence and acceptor absorption. The dynamic average value for isotropic systems $\kappa^2 = {}^2/_3$ was used.[40] The fluorescence quantum yield of the donor was adapted for the literature value ($\Phi_D = 0.75$).[16] The spectral overlap of the donor fluorescence band $f_D(\nu)$ (normalized to unity) with the absorption spectrum $\epsilon_A(\nu)$ of the acceptor was calculated to be $J = \int f_D(\nu)\, \epsilon_A(\nu) \nu^{-4} d\nu = 5.59 \times 10^{-14}$ cm^6 mol^{-1}. Thus, $R_0 = 44.6$ Å was obtained for the AO molecules. This value is comparable to the literature value of 37.0 Å for the AO in DNA solution.[15] To evaluate the energy transfer process, we estimate the rate constant which is represented by the following equation:[39]

$$k_{et} = \frac{1}{\tau_0}\left(\frac{R_0}{R}\right)^6 \quad (3)$$

To compare the τ_{dep} in the DNA matrix and k_{et}, the energy transfer associated with the depolarization in the observed range occurred between AO molecules at a distance in the range from 32 to 63 Å with $\tau_0 = 5.4$ ns and $R_0 = 37.0$ Å. The faster energy transfer occurs in less than 100 ps as a consequence of decrement of r_0 in which the intermolecular distance is ca. 20 Å, which is much shorter than the critical distance of 44.6 Å.

Amplified Quenching via the Excitation Energy Migration Process in Organized Media. In organized media such as the LB monolayer, the fluorescence lifetimes are shorter than that in the homogeneous solution. It is caused by the amplified quenching of the excited molecules via the excitation energy migration. The amplified quenching is applicable to the fluorescence sensor. For example, the squarylium dye LB films can detect NO_2 gas at the parts-per-billion level.[41] In our device combined with SPR excitation and DNA matrix, the NO_2 gas can be detected at 0.1 ppm level.[19] Recently Swager has proposed the "molecular wire" method for highly sensitive detection by the amplified quenching. The method is based on the energy or exciton migration along the π conjugated polymer.[42] The present method, on the other hand, does not use the π conjugated polymer but only a mixture of monomer dye and DNA solution. The methodology using the amplified quenching of dyes immobilized into DNA films is responsible for the sensing tool based on fluorescence detection by the present study. We develop the sensing devices using the DNA matrix in the field of amplified quenching via the highly efficient excitation energy migration.

Concluding Remarks

We investigated the fluorescence spectra, time-resolved fluorescence spectra, fluorescence lifetime, and fluorescence anisotropy decay of AO in DNA and PVA thin films to clarify the photophysical properties. To our knowledge these are the first observations of the efficient energy migration and amplified quenching of the dye intercalated into DNA thin films. The increscent of the fraction of AO results in a decrease of the fluorescence lifetime due to small amounts of trap sites. Time-resolved fluorescence depolarization measurement revealed that the excitation energy migration between AO became more efficient as the AO fraction increased. These findings indicate that the one-dimensional chain of DNA contributes to the

efficient energy migration between intercalated dyes. The present results also suggested that the fast responsive and highly sensitive chemical sensor device proposed by us is not only due to the improvement of the molecular dispersibility in DNA, but also to the amplified quenching followed by the efficient energy migration. The DNA matrix is adapted for the new devices using a fluorescence quenching response. The initial anisotropy value r_0 is decreasing with increasing fraction of AO, which implies that the much faster energy migration process occurs within the present time resolution. To clarify the fast process in the DNA films, we need to measure ultrafast dynamics by a fluorescence up-conversion method. The preparation of the LB monolayer is a tedious method compared to the preparation of DNA thin films, although both methods can gave well-organized systems. The similar behavior provides LB monolayers or the DNA films. The present result is not only important in the study of photochemical and photophysical properties of the dyes immobilized in DNA thin films but also throws light on the guidelines for the DNA photonics.

Acknowledgment. This work was partly supported by the 21st COE program "Functional Innovation of Molecular Informatics" of Kyushu University as well as the Grand-in-Aids for Encouragement of Young Scientist (B) (No. 18750015) and Research on Priority Areas (No. 17029047) "Fundamental Science and Technology of Photofunctional Interface" from the Ministry of Education, Culture, Sports, Science, and Technology (MEXT) of the Japanese government. F.I. also thanks the foundation Hattori-Hokokai for financial support.

Supporting Information Available: The time-resolved fluorescence spectra and fluorescence decay curves of AO in PVA films (PDF). This material is available free of charge via the Internet at http://pubs.acs.org.

Note Added after ASAP Publication. This article was published ASAP on April 18, 2007. One of the rows in Table 3 has been modified. The correct version was published on April 23, 2007.

References and Notes

(1) For example: (a) Cardullo, R. A.; Agrawal, S.; Flores, C.; Zamecnik, P. C.; Wolf, D. E. *Proc. Natl. Acad. Sci. U.S.A.* **1988**, *85*, 8790. (b) Kushon, S. A.; Ley, K. D.; Bradford, K.; Jones, R. M.; McBranch, D.; Whitten, D. *Langmuir* **2002**, *18*, 7245. (c) Liu, B.; Bazan, G. C. *Chem. Mater.* **2004**, *16*, 4467. (d) Ho, H. A.; Dore, K.; Boissinot, M.; Bergeron, M. G.; Tanguay, R. M.; Boudreau, D.; Leclerc, M. *J. Am. Chem. Soc.* **2005**, *127*, 12673.

(2) Weill, G.; Calvin, M. *Biopolymers* **1963**, *1*, 401.

(3) Hammes, G. G.; Hubbard, C. D. *J. Phys. Chem.* **1966**, *70*, 2889.

(4) Löber, G.; Achtert, G. *Biopolymers* **1969**, *8*, 595.

(5) Armstrong, R. W.; Kurucsev, T.; Stauss, U. P. *J. Am. Chem. Soc.* **1970**, *92*, 3174.

(6) Fredericq, E.; Houssier, C. *Biopolymers* **1972**, *11*, 2281.

(7) Kubota, Y. *Chem. Lett.* **1973**, 299.

(8) Schreiber, J. P.; Daune, M. P. *J. Mol. Biol.* **1974**, *83*, 487.

(9) Olmsted, J. III; Kearns, D. R. *Biochemistry* **1977**, *16*, 3647.

(10) Baguley, B. C.; Bret, M. L. *Biochemistry* **1984**, *23*, 937.

(11) Atherton, S. J.; Beaumont, P. C. *J. Phys. Chem.* **1987**, *91*, 3993.

(12) Brun, A. M.; Harriman, A. *J. Am. Chem. Soc.* **1992**, *114*, 3656.

(13) Brun, A. M.; Harriman, A. *J. Am. Chem. Soc.* **1994**, *116*, 10383.

(14) Atherton, S. J.; Beaumont, P. C. *J. Phys. Chem.* **1995**, *99*, 12025.

(15) Kubota, Y.; Steiner R. F. *Biophys. Chem.* **1977**, *6*, 279.

(16) Maliwal, B. P.; Kuśba, J.; Lakowicz, J. R. *Biopolymers* **1995**, *35*, 245.

(17) Kononov, A. I.; Moroshkina, E. B.; Tkachenko, N. V.; Lemmetyinen, H. *J. Phys. Chem. B* **2001**, *105*, 535.

(18) Fürstenberg, A.; Julliard, M. D.; Deligeorgiev, T. G.; Gadjev, N. I.; Vasilev, A. A.; Vauthey, E. *J. Am. Chem. Soc.* **2006**, *128*, 7661.

(19) Nagamura, T.; Yamamoto, M.; Terasawa, M.; Shiratori, K. *Appl. Phys. Lett.* **2003**, *83*, 803.

(20) Cho, H. S.; Rhee, H.; Song, J. K.; Min, C.-K.; Takase, M.; Aratani, N.; Cho, S.; Osuka, A.; Joo, T.; Kim, D. *J. Am. Chem. Soc.* **2003**, *125*, 5849.

(21) Sato, N.; Ito, S.; Sugiura, K.; Yamamoto, M. *J. Phys. Chem. A* **1999**, *103*, 3402.

(22) Lamm, M. E.; Neville, D. M. *J. Phys. Chem.* **1965**, *69*, 3872.

(23) Kurucsev, T.; Strauss, U. P. *J. Phys. Chem.* **1970**, *74*, 3081.

(24) (a) Kasha, M. *Radiat. Res.* **1963**, *20*, 55. (b) Kasha, M.; Rawls, H. R.; Ashraf El-Bayoumi, M. *Pure Appl. Chem.* **1965**, *11*, 371.

(25) Stomphorst, R. G.; Zwan, G.; Zandvoort, M. A. M. J.; Sieval, A. B.; Zuilhof, H.; Vergeldt, F. J.; Schaafsma, T. J. *J. Phys. Chem. A.* **2001**, *105*, 4235.

(26) Kimura, H.; Machida, S.; Horie, K.; Okahata, Y. *Polymer J.* **1998**, *30*, 708.

(27) Brauns, E. B.; Murphy, C. J.; Berg, M. A. *J. Am. Chem. Soc.* **1998**, *120*, 2449.

(28) Phillips, G. O.; Cundall, R. B.; Lewis, C.; Llewellyn, P. J. *J. Phys. Chem.* **1970**, *74*, 4172.

(29) Byrne, C. D.; Mello, A. J.; Barnes, W. L. *J. Phys. Chem. B* **1998**, *102*, 10326.

(30) Wilkinson, F.; Worrall, D. R.; Ferreira, L. F. V. *Spectrochimica Acta* **1992**, *48A*, 135.

(31) Yamazaki, I.; Tamai, N.; Yamazaki, T. *J. Phys. Chem.* **1990**, *94*, 516.

(32) Tamai, N.; Matsuo, H.; Yamazaki, T.; Yamazaki, I. *J. Phys. Chem.* **1992**, *96*, 6550.

(33) (a) Tamai, N.; Yamazaki, T.; Yamazaki, I. *Chem. Phys. Lett.* **1988**, *147*, 25. (b) Ichinose, N.; Nishimura, Y.; Yamazaki, I. *Chem. Phys. Lett.* **1992**, *197*, 364. (c) Yamazaki, I.; Tamai, N.; Yamazaki, T. *J. Phys. Chem.* **1987**, *91*, 3572.

(34) Nagamura, T.; Kamata, S.; Ogawa, T. *Nippon Kagaku Kaishi* **1987**, 2090.

(35) Nagamura, T.; Kamata, S.; Toyozawa, K.; Ogawa, T. *Ber. Bunsen-Ges. Phys. Chem.* **1990**, *94*, 87.

(36) Nagamura, T.; Toyozawa, K.; Kamata, S. *Colloids Surf. A* **1995**, *102*, 31.

(37) Yamazaki, I.; Yamaguchi, M.; Okada, N.; Akimoto, S.; Yamazaki, T.; Ohta, N. *J. Luminescence* **1997**, *72*−*74*, 71.

(38) Yang, J.; Roller, R. S.; Winnik, M. A. *J. Phys. Chem. B* **2006**, *110*, 11739.

(39) *Energy transfer parameters of aromatic compounds*; Berlman, I. B., Ed; Academic Press: New York, 1973.

(40) Lakowicz, J. R. *Principles of Fluorescence Spectroscopy*; Plenum Press: New York, 1983; pp 303−309.

(41) (a) Furuki, M.; Ageishi, K.; Kim, S.; Ando, I.; Pu, L. S. *Thin Solid Films* **1989**, *180*, 193. (b) Furuki, M.; Pu, L. S. *Thin Solid Films* **1992**, *210/211*, 471.

(42) (a) Swager, T. M. *Acc. Chem. Res.* **1998**, *31*, 201. (b) McQuade, D. T.; Pullen, A. E.; Swager, T. M. *Chem. Rev.* **2000**, *100*, 2537.